ISSN: 2476-6909; Modares. Mech. Eng. Eng. *2026;26(04):233-239.*

Modares Mechanical Engineering

DOI: 10.48311/mme.2026.118321.82912
journal homepage: mme.modares.ac.ir

Observer-Based Robust Disturbance Rejection for a Van der Pol Gyroscope Model

Seyed Ali Reza Hosseini, Mohammad Hassan Najjarnasab, Hassan Salarieh, Aria Alasti

Mechanical Engineering Department, Sharif University of technology, Tehran, Iran

ARTICLE INFO

Article Type
Original Research

Article History
Received: December 21, 2025
Revised: January 11, 2026
Accepted: January 16, 2026
ePublished: February 16, 2026

ABSTRACT

This paper addresses the robust control of a solid-state wave gyroscope (SSWG), modeled as a 2D Van der Pol oscillator. The objective is to achieve precise trajectory tracking in the presence of external disturbances and with reliance on estimated velocities. The performance of two sliding mode control (SMC) strategies using a high-gain observer (HGO) to estimate unmeasurable states is investigated and compared: a first-order Integral SMC (I-SMC) and a second-order Terminal Super-Twisting SMC (T-ST-SMC).

Simulation results demonstrate that while the I-SMC achieves tracking with laudable large disturbance rejection, it suffers from chattering in the control signal. In contrast, the T-ST-SMC provides a superior response by effectively mitigating chattering, yielding a smooth control action, enhanced error convergence, and greater robustness. Quantitative analysis reveals that the T-ST-SMC improves tracking accuracy by 46.5% and reduces control signal chattering by 39% compared to the I-SMC. A notable advantage of the T-ST-SMC is the elimination of the need to predefine an upper bound for disturbances.

The study concludes that the second-order T-ST-SMC offers a superior solution for the robust control of this SSWG model. It is demonstrated that the proposed feedback structure provides disturbance rejection under the condition of a defined, nonzero quadrature. As zero quadrature renders the control scheme flawed, the paper posits that for practical implementation, this control logic should be active when extreme quadrature values are present, and switching to an alternative quadrature suppression scheme when it approaches zero.

Keywords: 2D Van Der Pol Oscillator, Solid-State Wave Gyro, Terminal Super Twisting Sliding Mode, High-Gain Observer, Robust Disturbance Rejection, Unspecified Disturbance Bounds

How to cite this article
Hosseini S.A.R, Najjarnasab M.H, Salarieh H, Alasti A, Observer-Based Robust Disturbance Rejection for a Van der Pol Gyroscope Model. Modares Mechanical Engineering; *2026;26(04):233-239.*

**Corresponding author's email: salarieh@sharif.edu*
**Corresponding ORCID ID: 0000-0002-0604-5731*

1- Introduction

Inertial navigation is a fundamental technology for accurate and autonomous positioning. The successful operation of modern systems relies on the use of advanced navigation systems, which in turn depend on high-precision strapdown inertial navigation systems (SINS). It operates by using internal accelerometers and gyroscopes to continuously calculate a vehicle's position, velocity, and orientation. A gyroscope is a sensor that measures angular velocity. While various gyroscope technologies like dynamically-tuned gyros (DTG), ring laser gyros (RLG), and fiber optic gyros (FOG) are used, the Solid-State Wave Gyroscope (SSWG) stands out as a promising technology for future development [1,2,3].

The fundamental element of a SSWG is a high-quality piezoelectric or magneto-strictive solid-state waveguide, engineered to support the propagation of standing acoustic or spin waves. Unlike traditional gyroscopes with mechanical rotors, the SSWG utilizes elastic vibrations within its solid medium, where the waveguide is outfitted with transducers that monitor and control the wave vibrations. The operating principle relies on the inertia effect of these standing wave vibrations, detecting changes induced by rotation through the Coriolis effect on the wave patterns. This operational principle offers the advantage of engaging in elastic deformations without physical wear and tear, eliminating moving parts, subsequently increasing robustness, reliability and extending the device's operational life [4,5,6]. Research [7] demonstrates how the inherent geometrical nonlinearity of the resonator can be leveraged to naturally stabilize the gyroscope, combining the benefits of both positional resonant excitation and parametric resonance.

The behavior of these resonators is often studied using the Van der Pol oscillator as a mathematical model [8]. The evolution to two-dimensional (2D) and three-dimensional (3D) Van der Pol oscillator models has allowed for a more comprehensive understanding and control of the gyroscope's dynamics. Research by Zhuravlev [9] further explores this by constructing and proving the stability of a control system for an isotropic oscillator, ensuring that an elliptical trajectory with a non-zero quadrature is maintained. Achieving the high precision necessary for navigation-grade sensors requires effective control strategies. Recent advancements have focused on enhancing these strategies through improved mathematical modeling and robust control techniques. For instance, new regularization methods and scale factor analyses have been proposed to refine SSWG dynamics [10,11]. Furthermore, advanced approaches such as adaptive recursive terminal sliding mode control and disturbance observers have been developed to handle model uncertainties and improve tracking precision [12,13,14]. The goal of such control is to ensure the oscillator reaches a stable operational mode as quickly as possible. Research [15] has shown that feedback control based on the total energy of the oscillations is more effective than traditional amplitude-based feedback. A 2D oscillator, describes an elliptical trajectory in a plane. An extended 2D Van der Pol oscillator model with external control is now effectively used to study and enhance the performance of the new generation of SSWGs [16]. This concept has been extended to three dimensions [17], which propose a 3D integrating gyroscope based on the precession of standing waves in a spherically symmetric solid, likening it to a generalized Foucault pendulum.

In this paper, the feedback control scheme for a 2D van der pol oscillator proposed by Zhuravlev [16] is controlled using sliding mode control (SMC) algorithms subject to disturbance and operational limitations. First, the feedback control parameters are derived from the evolution of the dynamics of the extended 2D Van Der Pol oscillator, then, the control logic for two, dual input sliding mode variants is derived, integral SMC (I-SMC) and terminal super twisting SMC (T-ST-SMC) [18]. As subject to real-world applications, where only the deformations of the oscillator are observed, a high gain observer [19], upholding the separation principle, is put to use from the dynamics of the system and is incorporated within the control logic. At last, the design is put to test in simulation with the following constraints: the dynamics are updated every 0.001s, observation and control are carried out every 0.01s, saturation on the control inputs and an aggressive disturbance for a period to test robustness.

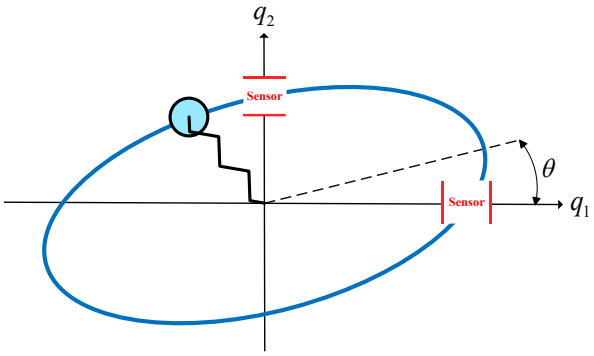

Fig. 1 2D van der pol oscillator.

2- Methodology

2-1- Deriving the basis of infinitesimal evolutions

The methodology presented here is from the works of Zhuravlev [8,9,15,16]. First, Consider the extended 2D Van Der Pol oscillator [16] with the form:

$$\begin{aligned} \ddot{q}_1 + q_1 &= \mu(1 - q_1^2 - q_2^2 - \dot{q}_1^2 - \dot{q}_2^2)\dot{q}_1 \\ \ddot{q}_2 + q_2 &= \mu(1 - q_1^2 - q_2^2 - \dot{q}_1^2 - \dot{q}_2^2)\dot{q}_2 \end{aligned} \tag{1}$$

With Energy and quadrature being:

$$\begin{aligned} E &= \frac{1}{2}(q_1^2 + q_2^2 + \dot{q}_1^2 + \dot{q}_2^2) \\ K &= q_1\dot{q}_2 - q_2\dot{q}_1 \end{aligned} \tag{2}$$

Proceed by writing the dynamics in the form:

$$\begin{aligned} \ddot{q}_1 + q_1 &= Q_1(q_1, q_2, \dot{q}_1, \dot{q}_2) \\ \ddot{q}_2 + q_2 &= Q_2(q_1, q_2, \dot{q}_1, \dot{q}_2) \end{aligned} \tag{3}$$

In free mode $(Q_1 = 0, Q_2 = 0)$, the oscillator describes an elliptical trajectory in the (q_1, q_2) plane with arbitrary principal semi-axes and arbitrary inclination of the major semi-axis relative to the q_1- axis which is depicted in Figure 1, regarding the electrode configuration in $0° - 45°$ placements.

Forces on the right-hand side of the (3) are interpreted as follows:

Perturbing forces: Deform the elliptical trajectory of free mode (changing semi-axis lengths, ellipse orientation, or disrupting its shape).

Control forces: Stabilize a given elliptical trajectory in a specific sense.

The general solution of (3) in free mode defines the parametric equations of the elliptical trajectory:

$$\begin{aligned} q_1 &= x_1 \cos t + x_3 \sin t \\ q_2 &= x_2 \cos t + x_4 \sin t \end{aligned} \tag{4}$$

The arbitrary constants (x_1, x_2, x_3, x_4) in (4) are treated as slow varying phase variables when $Q_1, Q_2 \neq 0$ and are small compared to the restoring force. Thus, the oscillation energy, angular momentum and ellipse area are:

$$E = \frac{1}{2}(x_1^2 + x_2^2 + x_3^2 + x_4^2) = \frac{1}{2}x^2 \tag{5}$$

$$K = x_1x_4 - x_2x_3 \tag{6}$$

$$\pi rk = \frac{1}{2}\int_0^{2\pi} (q_1\dot{q}_2 - q_2\dot{q}_1)dt = \pi K \tag{7}$$

where r is the major semi-axis and k is the minor semi-axis.

To correctly formulate feedbacks, controlling energy, quadrature, precession, or oscillation frequency, a basis for infinitesimal evolutions of the elliptical trajectory must be constructed.

A type of phase variables, known in celestial mechanics as *orbital elements* are proposed as $(q_1, q_2, \dot{q}_1, \dot{q}_2) \to (r, k, \theta, \tau)$:

$$\begin{aligned} q_1 &= r\cos(t+\tau)\cos\theta - k\sin(t+\tau)\sin\theta \\ q_2 &= r\cos(t+\tau)\sin\theta + k\sin(t+\tau)\cos\theta \end{aligned} \tag{8}$$

Where r is the Major semi-axis of the ellipse, k is the Minor semi-axis, θ is the Inclination angle of the major semi-axis to the q_1-axis and τ is the Initial position (at $t = 0$) of point (q_1, q_2) on the elliptical trajectory.

Rearranging, the slow variables are written as:

$$\begin{aligned} x_1 &= r\cos\tau\cos\theta - k\sin\tau\sin\theta \\ x_2 &= r\cos\tau\sin\theta + k\sin\tau\cos\theta \\ x_3 &= -r\sin\tau\cos\theta - k\cos\tau\sin\theta \\ x_4 &= -r\sin\tau\sin\theta + k\cos\tau\cos\theta \end{aligned} \tag{9}$$

Identification of the resonator parameters were carried out in a study [20], though not investigated as it is not in the scope of this paper. If $(Q_1, Q_2) = 0$, each ellipse in configuration space $q = (q_1, q_2)$ corresponds to a constant $x = (x_1, x_2, x_3, x_4)$ in phase space.

If $Q \neq 0$, the point $x(t)$ moves in phase space. In the configuration space $q = (q_1, q_2)$, this corresponds to evolution of the initial trajectory—ellipse or line segment. Analysis is carried out for a linear trajectory since in applications this is often required. Stabilizing elliptical trajectories with non-zero quadrature is essential for pendulum-type inertial navigation systems [8].

Four elementary evolutions exist:

- **Form precession**: Rotation of a line segment in the q-plane such that a rotating coordinate system exists where the segment is stationary.
- **Amplitude variation**: Change in segment length.
- **Frequency variation**: Change in oscillation frequency along a fixed segment.
- **Form disruption**: Evolution irreducible to the preceding evolutions.

Each evolution type corresponds to specific directions of $x(t)$ in phase space. Precession direction is formulated by Appling rotation $x \to y$ (angle α):

$$\begin{pmatrix} \cos\alpha & \sin\alpha \\ -\sin\alpha & \cos\alpha \end{pmatrix} \begin{pmatrix} x_1\cos t + x_3\sin t \\ x_2\cos t + x_4\sin t \end{pmatrix} = \begin{pmatrix} y_1\cos t + y_3\sin t \\ y_2\cos t + y_4\sin t \end{pmatrix} \tag{10}$$

$$e_1 = \frac{dy}{d\alpha}|_{\alpha=0} = \{x_2, -x_1, x_4, -x_3\}. \tag{11}$$

$$e_2 = \frac{dy}{d\mu}|_{\mu=0} = \{x_1, x_2, x_3, x_4\}. \tag{12}$$

$$e_3 = \frac{dK}{dx}|_{\tau=0} = \{x_4, -x_3, -x_2, x_1\}. \tag{13}$$

$$e_4 = \frac{dy}{d\tau}|_{\tau=0} = \{x_3, x_4, -x_1, -x_2\}. \tag{14}$$

Where (11-14) by order are precession, amplitude variation, Form disruption (quadrature), and Frequency change.

2-2- Deriving the Control scheme

Taking the derivative of (x_1, x_2, x_3, x_4), the explicit time-dependent resulting equation is averaged over time, yielding the general linear forces as:

$$\begin{pmatrix} Q_1 \\ Q_2 \end{pmatrix} = (C + N + H)\begin{pmatrix} q_1 \\ q_2 \end{pmatrix} + (D + \Gamma + G)\begin{pmatrix} \dot{q}_1 \\ \dot{q}_2 \end{pmatrix} \tag{15}$$

Table 1 Corresponding Forces

force	Precession(e_1)	Amplitude(e_2)	Quadrature(e_3)	Frequency(e_4)
C	0	0	0	$-c/2$
N	0	0	$-n/2$	**0**
D	0	$d/2$	0	**0**
Γ	$\gamma/2$	0	0	**0**

Where the matrices correspond to forces in the form of:

- C=cE Spherical potential.
- $N = n\begin{pmatrix} 0 & 1 \\ -1 & 0 \end{pmatrix}$ Circular.
- $H = h\begin{pmatrix} \cos 2\alpha & \sin 2\alpha \\ \sin 2\alpha & -\cos 2\alpha \end{pmatrix}$ Hyperbolic potential.
- D=dE Spherical dissipative.
- $\Gamma = \gamma\begin{pmatrix} 0 & 1 \\ -1 & 0 \end{pmatrix}$ Gyroscopic.
- $G = g\begin{pmatrix} \cos 2\beta & \sin 2\beta \\ \sin 2\beta & -\cos 2\beta \end{pmatrix}$ Hyperbolic dissipative.

H and G are unused in control. Mapping forces to $X(x)$:

$$C: -\frac{c}{2}e_4, \qquad N: -\frac{n}{2}e_3, \qquad D: \frac{d}{2}e_2, \qquad \Gamma = \frac{\gamma}{2}e_1 \tag{16}$$

Thus, as proposed by Zhuravlev [8], the control forces will be:

$$\left\|\begin{matrix} Q_1 \\ Q_2 \end{matrix}\right\| = d\left\|\begin{matrix} 1 & 0 \\ 0 & 1 \end{matrix}\right\|\left\|\begin{matrix} \dot{q}_1 \\ \dot{q}_2 \end{matrix}\right\| \tag{17}$$

$$\left\|\begin{matrix} Q_1 \\ Q_2 \end{matrix}\right\| = c\left\|\begin{matrix} 1 & 0 \\ 0 & 1 \end{matrix}\right\|\left\|\begin{matrix} q_1 \\ q_2 \end{matrix}\right\| \tag{18}$$

$$\left\|\begin{matrix} Q_1 \\ Q_2 \end{matrix}\right\| = \gamma\left\|\begin{matrix} 0 & 1 \\ -1 & 0 \end{matrix}\right\|\left\|\begin{matrix} \dot{q}_1 \\ \dot{q}_2 \end{matrix}\right\| \tag{19}$$

$$\left\|\begin{matrix} Q_1 \\ Q_2 \end{matrix}\right\| = n\left\|\begin{matrix} 0 & 1 \\ -1 & 0 \end{matrix}\right\|\left\|\begin{matrix} q_1 \\ q_2 \end{matrix}\right\| \tag{20}$$

Where by order, the forces are total vibration energy stabilization (amplitude), frequency control, precession control and quadrature stabilization. the parameters n & d are:

$$n = \mu_2\frac{K}{E} \quad d = \mu_3(1 - 2E) \tag{21}$$

Thus, taking the feedback Control forces into account and incorporating them to the dynamics (1):

$$\begin{aligned} \ddot{q}_1 + q_1 &= \acute{\mu}_3\left(\frac{1}{2} - E\right)\dot{q}_1 - \mu_2\frac{K}{E}q_2 - \gamma\dot{q}_2 + cq_1 \\ \ddot{q}_2 + q_2 &= \acute{\mu}_3\left(\frac{1}{2} - E\right)\dot{q}_2 + \mu_2\frac{K}{E}q_1 + \gamma\dot{q}_1 + cq_2 \end{aligned} \tag{22}$$

Where $\acute{\mu}_3 = \frac{\mu - \mu_3}{2}$ is interpreted as a constant energy feedback subtraction parameter corresponding to an amplitude control scheme which is not investigated here. A study was carried out [5] suggesting that the precession angle θ grows linearly with γ which is an obvious claim regarding the provenance of the physical phenomena. If it is necessary to provide a given precession of the oscillation form with an angular velocity ω, then $\gamma = \mu_4(\omega - \dot{\theta})$.

3- Basis of Control using sliding mode

The motive for controlling this scheme provided by Zhuravlev [16] is that the γ parameter introduces an imbedded external disturbance into our dynamic, namely, the induced angular velocity which it's sensing is the purpose of the SSWG.

We seek to have the 2D oscillator track the solution to $\ddot{q} + q = 0$ for given initial conditions regarding a tolerable bound for quadrature, with robustness to an unknown parameter γ within a predefined bound, which is a nonlinear tracking control problem of preserving a desired amplitude and frequency.

In this study, suitable variants of SMC are implemented and tuned in accordance to the problem definition. For emulating the reality of the problem, the model dynamic is updated every 0.001s and the control input and observation are carried out every 0.01s, and for robustness evaluation, from 10s to 10.5s, 25s to 25.5s, 40s to 40.5s, the disturbance takes aggressive values which were not expected for in

the control scheme, and a saturation bound constrains the final control output.

Among the feedback forces which form (22), $\acute{\mu}_3$ could be interpreted as a constant value, resultant of feedbacking the Energy model of the system back into the extended 2D van der pol equations. γ is the direct result of external rotation of the system and interpreted as disturbance, as the goal is to keep the oscillator tracking a stationary predefined trajectory. The other two feedback forms left, namely c and μ_2 are taken as the control input due to both being explicit external feedbacks and having a relatively workable structure, all the while perceiving μ_2 as a robustness parameter and an embedded quadrature regulation factor, as the structure of this feedback dynamic is sensitive to aggressive quadrature values.

3-1- Sliding mode control derivation for the given dynamics

The system is quadratic (two inputs and two dynamic blocks); thus, the equations are derived as follows:

$$\ddot{q}_1 = f_1(X) + \sum_{j=1}^{2} g_{1j}(X)u_j$$
$$\ddot{q}_2 = f_2(X) + \sum_{j=1}^{2} g_{2j}(X)u_j \tag{23}$$

$$\bar{q}^{(2)} = f(X) + Gu \tag{24}$$

Where:

$$f = \begin{bmatrix} f_1(X) \\ f_2(X) \end{bmatrix} = \begin{bmatrix} \acute{\mu}_3\left(\frac{1}{2} - E\right)\dot{q}_1 - \gamma\dot{q}_2 - q_1 \\ \acute{\mu}_3\left(\frac{1}{2} - E\right)\dot{q}_2 + \gamma\dot{q}_1 - q_2 \end{bmatrix} \tag{25}$$

$$\hat{f} = \begin{bmatrix} \acute{\mu}_3\left(\frac{1}{2} - E\right)\dot{q}_1 - q_1 \\ \acute{\mu}_3\left(\frac{1}{2} - E\right)\dot{q}_2 - q_2 \end{bmatrix} \tag{26}$$

$$F = |f - \hat{f}| = \gamma_{max}\begin{bmatrix} |\dot{q}_2| \\ |\dot{q}_1| \end{bmatrix} \tag{27}$$

$$G = \begin{bmatrix} g_{11} & g_{12} \\ g_{21} & g_{22} \end{bmatrix} = \begin{bmatrix} q_1 & -\frac{K}{E}q_2 \\ q_2 & \frac{K}{E}q_1 \end{bmatrix} \quad u = \begin{bmatrix} c \\ \mu_2 \end{bmatrix} \tag{28}$$

With Integral and Terminal sliding surfaces by order:

$$\tilde{x}_{1,2} = q_{1,2} - q_{desired_{1,2}} \tag{29}$$

$$s_i = \left(\frac{d}{dt} + \lambda_i\right)^2 \int_0^t \tilde{x}_i\, dt \rightarrow s_{1,2} = \dot{\tilde{x}}_{1,2} + +2\lambda_{1,2}\tilde{x}_{1,2} + \lambda_{1,2}^2\int_0^t \tilde{x}_i\, dt - \dot{\tilde{x}}_{1,2}(0) - 2\lambda_{1,2}\tilde{x}_{1,2}(0) \tag{30}$$

$$s_{1,2} = \dot{\tilde{x}}_{1,2} + \beta\tilde{x}_{1,2}^{\frac{p}{q}} = \dot{\tilde{x}}_{1,2} + \beta sign(\tilde{x}_{1,2})|\tilde{x}_{1,2}|^{\frac{p}{q}} \tag{31}$$

The Lyapunov candidate function is introduced as:

$$V = \frac{1}{2}s^2 \rightarrow \frac{d}{dt}(V) = s\dot{s} \leq -\eta|s| \tag{32}$$

Where with trivial derivation, the control logics are as:

- Integrator with a continuous switching law:

$$u = G^{-1}\left(-\hat{f} + \ddot{q}_{desired_{1,2}} - 2\lambda_{1,2}\dot{\tilde{x}}_{1,2} - u_{switch-I} - \lambda_{1,2}^2(\tilde{x}_{1,2} - \tilde{x}_{1,2}(0))\right)$$
$$u_{switch-I} = \begin{bmatrix} K_1 sat(s_1/\phi) \\ K_2 sat(s_2/\phi) \end{bmatrix} \tag{33}$$
$$K_{1,2} \geq F + \eta_{1,2}$$

- Terminal Super Twisting with a small parameter $\epsilon = 0.01$ to prevent singularity:

$$u = G^{-1}\left(-\hat{f} + \ddot{q}_{desired_{1,2}} - \frac{\beta p}{q}\dot{\tilde{x}}_{1,2}(|\tilde{x}_{1,2}|^{\frac{p}{q}-1} + \epsilon) - u_{switch-T}\right)$$
$$u_{switch-ST} = \begin{bmatrix} k_1\sqrt{s_1}sat(s_1/\phi) + k_2\int_0^\tau sign(s_1)d\tau \\ k_1\sqrt{s_2}sat(s_2/\phi) + k_2\int_0^\tau sign(s_2)d\tau \end{bmatrix} \tag{34}$$

3-2- HGO for attaining the dimensionless velocities

In real applications, online values of q_1& q_2 are observed, but the values of $\dot{q}_1$ & $\dot{q}_2$ which are explicitly utilized in the control schemes (33) & (34) are not directly accessible. For the purpose of attaining these two states and with respect to the scheme of the dynamic model (22), a high gain observer (HGO) [19] is proposed. The advantage of using this observer is that it holds the principle of separation of estimation and control. This validity arises from the singular perturbation nature of High-Gain Observers; for sufficiently high gains, the observer error dynamics become fast enough to be time-scale separated from the slower system kinetics, effectively recovering the performance of the state feedback controller [19], leaving the proposed controlled scheme (22) unhinged in terms of stability analysis by the additional nonlinear observer.

The HGO is proceeded by:

$$Z = \begin{bmatrix} z_1 \\ z_2 \\ z_3 \\ z_4 \end{bmatrix} = \begin{bmatrix} q_1 \\ q_2 \\ \dot{q}_1 \\ \dot{q}_2 \end{bmatrix} \tag{35}$$

$$\dot{z}_3 + z_1 = U_1(z_1, z_2, z_3, z_4, \acute{\mu}_3, \mu_2, \gamma, c)$$
$$\dot{z}_4 + z_2 = U_2(z_1, z_2, z_3, z_4, \acute{\mu}_3, \mu_2, \gamma, c) \tag{36}$$

With the observations as:

$$y = \begin{bmatrix} z_1 \\ z_2 \end{bmatrix} \tag{37}$$

$$\dot{Z} = \begin{bmatrix} z_3 \\ z_4 \\ U_1 - z_1 \\ U_2 - z_2 \end{bmatrix} = f(Z, U) \tag{38}$$

$$\dot{\hat{Z}} = f(\hat{Z}, U) + H(y - \hat{y}) \tag{39}$$

$$H = \begin{bmatrix} \frac{\alpha_1}{\epsilon} & 0 \\ 0 & \frac{\alpha_1}{\epsilon} \\ \frac{\alpha_2}{\epsilon^2} & 0 \\ 0 & \frac{\alpha_2}{\epsilon^2} \end{bmatrix} \tag{40}$$

Where $0 < \epsilon < 1$ is the tuning parameter and the α_1, α_2 coefficients are chosen so that $s^2 + \alpha_2 s + \alpha_1 = 0$ is Hurwitz.

The observer dynamics will be:

$$\dot{\hat{z}}_1 = \hat{z}_3 + \frac{\alpha_1}{\epsilon}(y_1 - \hat{z}_1)$$
$$\dot{\hat{z}}_2 = \hat{z}_4 + \frac{\alpha_1}{\epsilon}(y_2 - \hat{z}_2)$$
$$\dot{\hat{z}}_3 = -\hat{z}_1 + \hat{U}_1(\hat{Z}, \acute{\mu}_3, \mu_2, c) + \frac{\alpha_2}{\epsilon^2}(y_1 - \hat{z}_1) \tag{41}$$
$$\dot{\hat{z}}_4 = -\hat{z}_2 + \hat{U}_2(\hat{Z}, \acute{\mu}_3, \mu_2, c) + \frac{\alpha_2}{\epsilon^2}(y_2 - \hat{z}_2)$$

And the estimation error as:

$$\dot{e} = \begin{bmatrix} e_3 - \frac{\alpha_1}{\epsilon}e_1 \\ e_4 - \frac{\alpha_1}{\epsilon}e_2 \\ \delta_1 - \frac{\alpha_2}{\epsilon^2}e_1 \\ \delta_2 - \frac{\alpha_2}{\epsilon^2}e_2 \end{bmatrix} \tag{42}$$

$$\Delta = \begin{bmatrix} \delta_1 \\ \delta_2 \end{bmatrix} = \begin{bmatrix} U_1(Z, \acute{\mu}_3, \mu_2, \gamma, c) - \hat{U}_1(\hat{Z}, \acute{\mu}_3, \mu_2, c) \\ U_2(Z, \acute{\mu}_3, \mu_2, \gamma, c) - \hat{U}_2(\hat{Z}, \acute{\mu}_3, \mu_2, c) \end{bmatrix} \tag{43}$$

4- Simulation results

The parameters of energy feedback $\mu_3 = \frac{1}{2}$, HGO $\alpha_1 = 1$, $\alpha_2 = 2$, $\epsilon = 0.05$, controller saturation limit as 25, $\phi = 0.5$ and the disturbance γ which is:

$$\gamma = \begin{cases} 0 & t < 5s \\ 150\sin(100t) & 10s, 25s, 40s, half\ a\ second \\ 2\sin(100t) & all\ other\ t \end{cases} \quad (44)$$

are all held constant across both simulations. This specific signal volatility in the disturbance is what the system showed the most sensitivity to, thus implemented to conduct the disturbance rejection study. The predefined disturbance bound $\gamma_{max} = 3$ is introduced for the I-SMC. The controller and observer activation time is every 0.01s, and the dynamic's update time is every 0.001s.

A quantitative measure for relative performance is introduced as:

$$P = \frac{\sum_{t=0}^{T} \|\zeta\|_1^{I-SMC} - \|\zeta\|_1^{T-ST-SMC}}{\sum_{t=0}^{T} \|\zeta\|_1^{I-SMC}} \quad (45)$$

Where $\zeta = e(t); \Delta u(t)$. Tracking accuracy is evaluated using the accumulated error norm, while chattering intensity is assessed by summing the magnitude of changes in the control effort between consecutive steps. The primary objectives are to achieve robust reference tracking despite external disturbances and to rely solely on observable system states by using an HGO.

Figure 2 illustrates the performance of the I-SMC. The reference tracking error, shown in Figure 2(a), demonstrates that the controller effectively forces the system states to follow the desired trajectory up to some extent of an oscillating error. However, noticeable deviations in tracking error occur during the aggressive disturbance periods (10-10.5s, 25-25.5s, and 40-40.5s) which is also present for the T-ST-SMC case. The control inputs, depicted in Figure 2(b), exhibit significant chattering. This high-frequency switching is a known characteristic of first-order sliding mode control. The control effort also reaches the saturation limit of 25 during the disturbance intervals, indicating the controller is working at its maximum capacity to counteract these events. The sliding surfaces for the I-SMC, seen in Figure 4(a), show that the system trajectories are driven to and maintained on the sliding manifold, although with some oscillation, particularly when large disturbances are introduced. A key deficiency of I-SMC here is pre defining the disturbance bound γ, which is not present for the T-ST-SMC.

The T-ST-SMC's performance, detailed in Figure 3, presents a more refined control action. The reference tracking errors in Figure 3(a) are visibly smaller than those of the I-SMC. This suggests a higher degree of robustness. A significant advantage of the T-ST-SMC is the reduction in chattering, as seen in the control effort plot in Figure 3(b). The super-twisting algorithm, a second-order sliding mode technique, smooths the control signal by integrating the discontinuous term, leading to a continuous control action that is more practical for implementation. While the control inputs are still highly active, the high-frequency oscillations are less pronounced compared to the I-SMC.

As was the incentive of the study to delineate robustness of the said control logics to large external disturbances, both SMCs depicted close, acceptable behavior. In further investigation of SMC variant's result discrepancies, it is observed that the T-ST-SMC yielded a 46.5% improvement in tracking accuracy and a 39% reduction in control signal chattering relative to the I-SMC.

Figure 3(c) highlights the controller's ability to manage the quadrature evolution, keeping it close to the reference value even in the presence of disturbances. This is crucial for the proper function of the gyroscope model. The observer performance error which is consistent for both cases, shown in Figure 3(d), remains bounded and relatively small, validating the effectiveness of the High-Gain Observer in estimating the unmeasurable states. The sliding surfaces for the T-ST-SMC in Figure 4(b) appear smoother than those for the I-SMC, indicating a more stable and less agitated response on the sliding manifold. The terminal sliding mode aspect of this controller is designed to ensure faster, finite-time convergence of the tracking error.

Table 2 Simulation control parameters

SMC/ Params	$p-q$	β	k_1, k_2	$\lambda_{1,2}, \eta_{1,2}$
ISMC	-	-	-	**3.5-10**
T-ST-SMC	6-5	12.5	9-2	-

5- Conclusion

This study successfully demonstrated the robust control of a 2D Van der Pol oscillator model for a SSWG. The control objective was to ensure precise trajectory tracking subject to a bounded, defined, nonzero quadrature in the presence of significant external disturbances and with reliance on estimated velocities.

As it is apparent with respect to the figures and the quantitative evaluation in the discussion, both I-SMC and T-ST-SMC achieved tracking with robustness to large disturbances. Although both logics had marginally similar behavior in response to the large disturbances, the T-ST-SMC demonstrated a better performance in terms of overall tracking precision and control input smoothness. The first-order I-SMC exhibited sharp, high-frequency input variations, known as chattering, and struggled to completely suppress its sliding surfaces. In contrast, the second-order T-ST-SMC effectively mitigated these issues, providing a smooth and continuous control signal while demonstrating superior error handling and convergence on the sliding surfaces. Quantitatively, this proposed strategy yielded a 46.5% improvement in tracking accuracy and a 39% reduction in control signal chattering relative to the I-SMC. A core advantage of the terminal super twisting variant over the I-SMC is the elimination of the need to predefine a disturbance bound γ_{max} during the implementation of the control logic. Despite this, the T-ST-SMC showcased comparatively superb performance, indicating a higher degree of robustness in implementation.

In conclusion, this work demonstrates that second-order SMC, and particularly the Terminal Super-Twisting variant, offers a superior solution for the robust control of SSWGs subject to large disturbances. It successfully addresses the dual challenges of aggressive external disturbance rejection and chattering elimination while operating with estimated states. The claim is that in accordance to the proposed feedbacks, if a defined nonzero quadrature; as zero quadrature renders this papers control scheme deficient as only one input remains subject to the assumptions made; is tolerated for a period before switching to conventional solutions for quadrature mitigation in literature, this closed loop system rejects disturbances with precision, obliged to the contribution of the feedback with the form $\mu_2 \frac{K}{E} q_n$.

Future work could involve applying perturbation analysis methods to further investigate the analytical properties of the feedback forms. Additionally, the extension of the control framework to three-dimensional models and the integration of adaptive observation schemes may be considered.

Ethics Approval:

The scientific content of this article is the result of the authors' research and has not been published in any Iranian or international journal.

Conflict of Interest:

There are no conflicts of interest to declare.

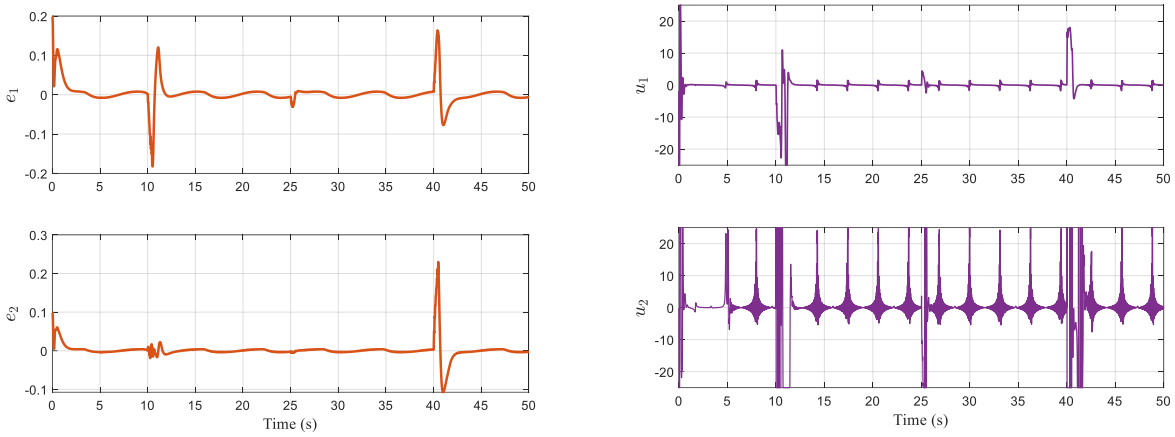

(a) **(b)**

Fig.2 I-SMC - (a) reference tracking error (b) control inputs

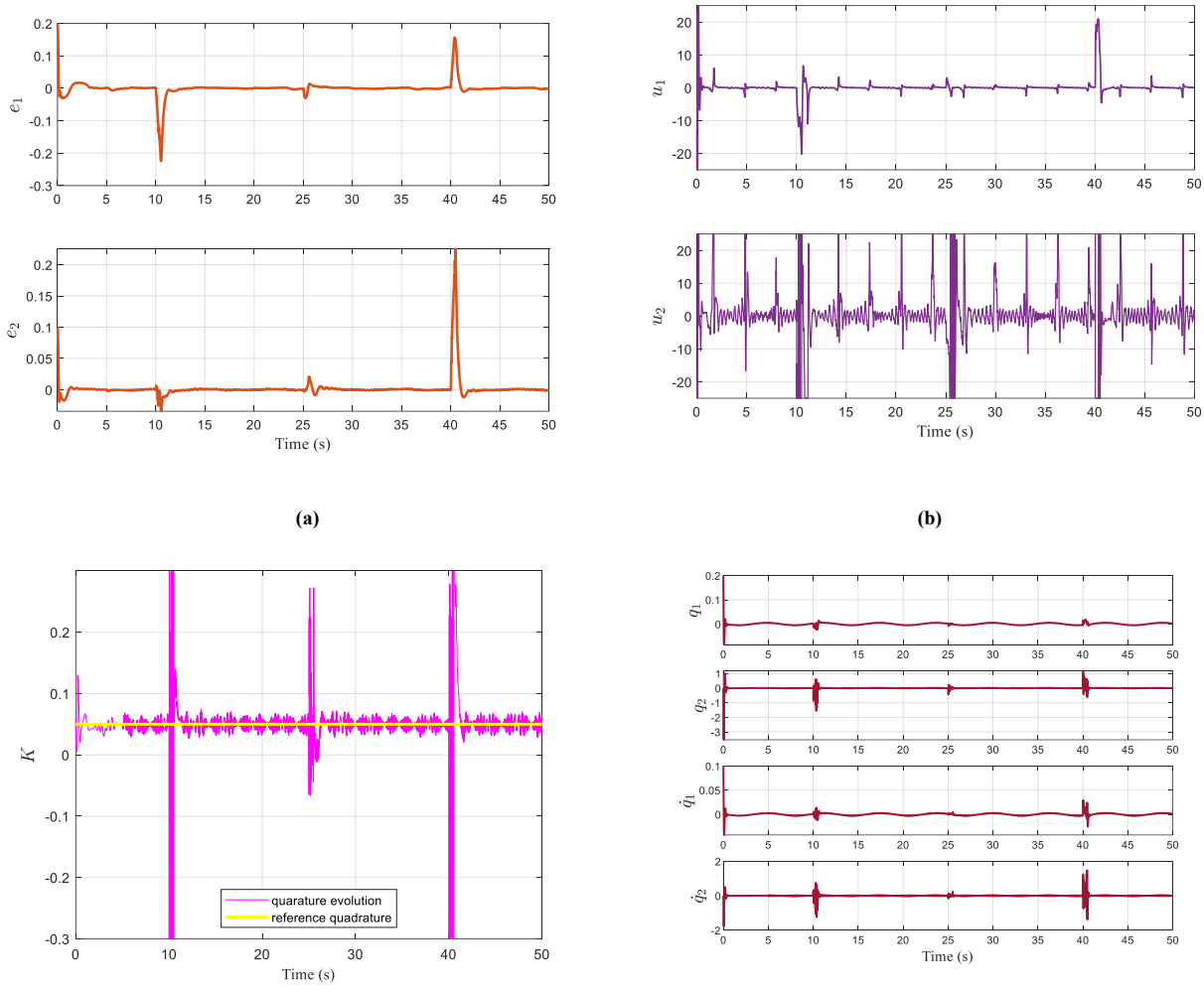

(a) **(b)**

(c) **(d)**

Fig.3 T-ST-SMC - **(a)** reference tracking errors **(b)** control effort **(c)** quadrature evolution **(d)** observer performance error.

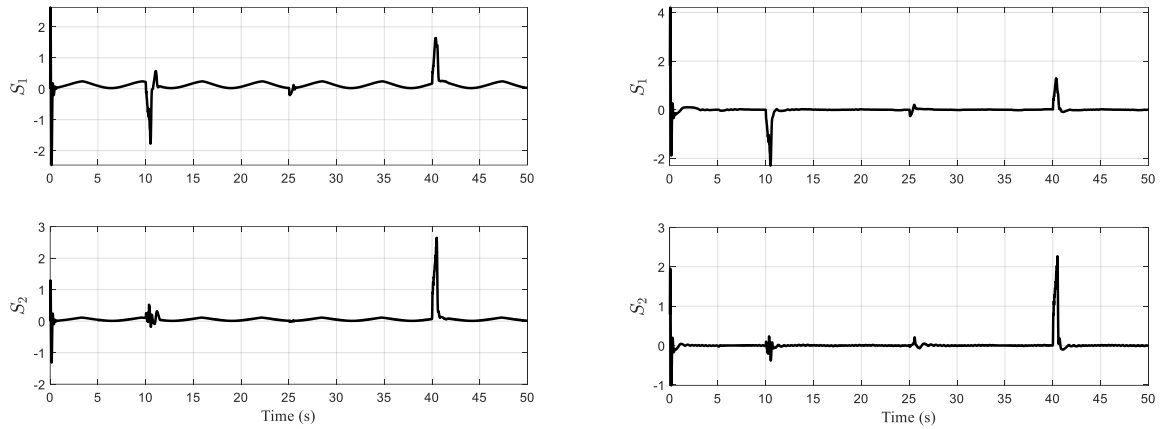

(a) **(b)**

Fig.4 Sliding surfaces – (a) I-SMC (b) T-ST-SMC.

References

[1] A. A. Maslov, D. A. Maslov, I. G. Ninalalov, and I. V. Merkuryev, "Hemispherical Resonator Gyros (An Overview of Publications)," *Gyroscopy and Navigation*, vol. 14, no. 1, pp. 1–13, 2023. doi: 10.1134/s2075108723010054

[2] V. Ph. Zhuravlev, S. E. Perelyaev, B. P. Bodunov, and S. B. Bodunov, "New-Generation Small-Size Solid-State Wave Gyroscope for Strapdown Inertial Navigation Systems of Unmanned Aerial Vehicle" in *Proc. 24th Saint Petersburg International Conference on Integrated Navigation Systems (ICINS)*, 2017. doi: 10.23919/ICINS.2019.8769344

[3] S.E. Perelyaev, S.B. Bodunov, and B.P. Bodunov, "Navigation Grade Solid-State Wave Gyro for Air-Space Applications" in *2022 29th Saint Petersburg International Conference on Integrated Navigation Systems (ICINS)*, Saint Petersburg, Russia, 2022, pp. 1-7. doi: 10.23919/ICINS51784.2022.9815352

[4] S.E. Perelyaev and B.P. Bodunov, "Solid-state wave gyroscope: A new-generation inertial sensor" in Proc. 24th Saint Petersburg International Conference on Integrated Navigation Systems (ICINS), 2017. doi: 10.23919/ICINS.2017.7995651

[5] Y. Tao, X. Xiang, and Y. Wu, "Design, Analysis and Experiment of a Novel Ring Vibratory Gyroscope" in 2011 IEEE International Conference on Mechatronics and Automation (ICMA), 2011, pp. doi: 10.1016/j.sna.2011.04.039

[6] T. Yi, "A Novel Cupped Solid-State Wave Gyroscope" in Proc. Trans Tech Publications Ltd., 2012. doi: 10.4028/www.scientific.net/AMM.110-116.715

[7] D. A. Kovriguine, "Geometrical nonlinearity stabilizes a wave solid-state gyro" *Archive of Applied Mechanics*, vol. 84, no. 2, pp. 159–172, 2014. doi: 10.1007/s00419-013-0791-0

[8] V. F. Zhuravlev, "Van der Pol's controlled 2D oscillator" *Rus. J. Nonlin. Dyn.*, vol. 12, no. 2, pp. 211–222, 2016.K. Elissa.

[9] V. Ph. Zhuravlev, "On the Stability of Control of an Inertial Pendulum-Type System" *Mechanics of Solids*, vol. 53, no. 5, pp. 489–491, 2018. doi: 10.3103/S002565441808022

[10] D. A. Maslov, "The holomorphic regularization method of the Tikhonov system of differential equations for mathematical modeling of wave solid-state gyroscope dynamics," Russian Journal of Nonlinear Dynamics, vol. 21, no. 2, pp. 233–248, 2025. doi: 10.20537/nd250211

[11] A. A. Maslov, D. A. Maslov, and I. V. Merkuryev, "Scale factor of the solid-state wave gyroscope operating in the mode of a compensation-type angular rate sensor," Gyroscopy and Navigation, vol. 15, no. 4, pp. 297–304, Mar. 2025. doi: 10.1134/S207510872570004

[12] L. Laiwu, X. Chen, and Y. Liu, "Adaptive recursive terminal sliding mode control for MEMS gyros using improved neural network with constrained input mapping," IEEE Access, vol. 13, pp. 71930–71942, 2025. doi: 10.1109/ACCESS.2024.3511234

[13] R. Zhang, B. Xu, S. Li, and G. Gao, "Recursive integral terminal sliding mode control with combined extended state observer and adaptive Kalman filter for MEMS gyroscopes," Microsystem Technologies, vol. 30, no. 2, pp. 1–12, 2024. doi: 10.1007/s00542-023-05512-9

[14] Z. Wen, Y. Zhang, and H. Wang, "Sliding mode control for MEMS gyroscopes using modified neural disturbance observer," in 2024 36th Chinese Control and Decision Conference (CCDC), IEEE, pp. 1245–1250, May 2024. doi: 10.1109/CCDC58219.2024.10619876

[15] V. F. Zhuravlev, "On the Formation of Feedbacks in the Van der Pol Spatial Oscillator" *Mechanics of Solids*, vol. 55, no. 7, pp. 926–931, 2020. doi: 10.3103/S0025654420070213

[16] V. Ph. Zhuravlev, "Van der Pol Oscillator. Technical Applications" *Mechanics of Solids*, vol. 55, no. 1, pp. 132–137, 2020. doi: 10.3103/S0025654420010203

[17] V. Zhuravlev, S. Perelyaev, and D. Borodulin, "The Generalized Foucault Pendulum is a 3D Integrating Gyroscopes Using the Three-Dimensional Precession of Standing Waves in a Rotating Spherically Symmetric Elastic Solid" in *2019 DGON Inertial Sensors and Systems (ISS)*, Braunschweig, Germany, 2019, pp. 1-12. doi: 10.1109/ISS46986.2019.8943687

[18] Y. Shtessel, C. Edwards, L. Fridman, and A. Levant, *Sliding Mode Control and Observation*. New York: Springer, 2014.

[19] H. K. Khalil, *Nonlinear Systems*, 3rd ed. Upper Saddle River, NJ: Prentice Hall, 2002.

[20] R. I. Mingazov, F. I. Spiridonov, I. A. Vikhlyaev, and K. V. Shishakov, "Comparison of Methods for Determining the Physical Parameters of the Resonator of a Solid-State Wave Gyroscope" in *Proceedings of the VI International Forum "Instrumentation Engineering, Electronics and Telecommunications - 2020"*, Izhevsk, Russian Federation, 2020, pp. 6-11. doi: 10.22213/2658-3658-2020-6-11